

Fabrication of reduction-degradable micelle based on disulfide-linked graft copolymer-camptothecin conjugate for enhancing solubility and stability of camptothecin

Honglei Fan^a, Jin Huang^{a,b,*}, Yaping Li^c, Jiahui Yu^{b,**}, Jinghua Chen^d

^a College of Chemical Engineering, Wuhan University of Technology, Wuhan 430070, PR China

^b Institutes for Advanced Interdisciplinary Research, East China Normal University, Shanghai 200062, PR China

^c Center for Drug Delivery System, Shanghai Institute of Materia Medica, Chinese Academy of Sciences, Shanghai 201203, PR China

^d School of Medicine and Pharmaceutics, Jiangnan University, Wuxi 214122, PR China

ARTICLE INFO

Article history:

Received 4 June 2010

Received in revised form

17 August 2010

Accepted 1 September 2010

Available online 15 September 2010

Keywords:

Reduction-degradable

Camptothecin

Micelle

ABSTRACT

This research is aimed to develop a reduction-degradable micelle delivery system based on polymer-camptothecin (CPT) conjugate in order to enhance the solubility and stability of CPT in aqueous media. Firstly, disulfide-linked poly(amido amine) (SS-PAA) containing alkyne groups was synthesized by Michael addition polymerization between propargyl amine and *N,N'*-bis(acryloyl) cystamine (BAC). And then, azide-functionalized CPT derivatives were conjugated with SS-PAA by click cycloaddition. Further grafting of residual alkyne groups in SS-PAA with azide-terminated poly(ethylene glycol) methyl ether (mPEG) gave mPEG-*g*-SS-PAA-CPT conjugate. At last, micelles with size of ca. 88 nm were fabricated from mPEG-*g*-SS-PAA-CPT conjugate, suggesting their passive targeting potential to tumor tissue. It was worthy of note that the drug-loaded system of mPEG-*g*-SS-PAA-CPT micelles improved the solubility and stability of CPT in aqueous media. Owing to the reduction degradability of disulfide linker in main chain of polymer in the presence of dithiothreitol (DTT), the CPT sustainably release from micelles together with the gradual cleavage of polymer at the concentration of simulating the intracellular condition while almost no change occurred at the level of DTT corresponding to extracellular condition. Furthermore, the cell viability results showed the essential decrease of cytotoxicity to L929 cell line. These results present a strategy in designing anti-tumor CPT-polymer conjugates for highly selective delivery to tumor cells.

© 2010 Elsevier Ltd. All rights reserved.

1. Introduction

Besides the traditional intelligent drug carriers based on the temperature- and pH-sensitive micelles and polymersomes [1–3], the reduction-response biodegradable polymers have emerged as a fascinating class of drug-loading materials [4], in the forms of drug-conjugate [5,6], nano/micro-gel [7,8] and micelle [9,10], for intracellular triggered delivery and release of protein and low-molecular-weight drug. In the view of molecular level, the disulfide linkage is the typical character of these reduction-sensitive

polymers, and usually locates in main chain, side chain or cross-linker. A notable fact has been found that the cleavage of disulfide linkage, due to the thiol-disulfide exchange reaction, is sensitive to the reduction conditions in human body. In the body circulation and the extracellular milieu, the disulfide bonds showed enough stability to a low concentration of glutathione tripeptide (GSH) as ca. 2–20 μ M. However, the intracellular high concentration of GSH (0.5–10 mM) can lead to the quick degradation of disulfide-linked polymers. As a result, the drugs conjugated or encapsulated with these reducible polymers are destined for intracellular delivery and release. In addition, these reduction-response polymers are especially suitable for the triggered delivery of tumor-specific drug because of the higher concentration of GSH in tumor tissue at least 4-fold over normal tissues [4].

20(*S*)-Camptothecin (CPT), a pentacyclic alkaloid isolated from the Chinese tree *Camptotheca acuminata* [11], has been verified as a broad range of anti-cancer activity in animal models [12]. However, both low solubility in aqueous medium and ring-

* Corresponding author. College of Chemical Engineering, Wuhan University of Technology, Wuhan 430070, PR China. Tel.: +86 27 63373510; fax: +86 27 87859019.

** Corresponding author.

E-mail addresses: huangjin@iccas.ac.cn (J. Huang), jhyu@sist.ecnu.edu.cn (J. Yu).

opening of active lactone at physiological pH, as well as high toxicity, greatly limit its clinical application [13,14]. It is known that a pH-dependent equilibrium between lactone form and carboxylate form in aqueous solution for CPT (Fig. 1) results in the inactive carboxylate form of most CPT molecules at physiological pH, and hence produces bone marrow and nonhematologic toxicities. On the other hand, the closed lactone ring (E-ring) of CPT is essential for its anti-tumor activity [15,16]. The 20-OH group of the E-ring of CPT is necessary for ring opening, and can participate into the enhanced rate of lactone hydrolysis at physiological pH. At the same time, serum albumin preferentially binds the carboxylate form of CPT to shift the lactone/carboxylate equilibrium in favor of the carboxylate form [17,18]. As a result, acylation of the 20-OH group has been verified to inhibit the participation of lactone hydrolysis, and hence significantly enhanced the stability of the E-ring of CPT. Meanwhile, 20-O-acylated CPT possesses no intrinsic topoisomerase I inhibitory activity [19–21]. Currently, it become popular that the 20-OH of CPT is covalently conjugated with water-soluble polymer, such as polyethylene glycol (PEG) [21], poly(L-glutamic acid) (PGA) [22], β -cyclodextrin based polymers [23], poly(1-hydroxymethyl-ethylene hydroxyl-methyl formal) [24], poly[N-(2-hydroxypropyl) methacrylamide] (HPMA) [25], α,β -poly[(N-carboxybutyl)-L-aspartamide] (PBAsp) [26], and so on. This not only enhanced the stability of CPT in the active lactone form, but also improved its water-solubility. In this case, the release of CPT was under control by the hydrolysis of ester bonds between polymer and CPT. It has been found that the PGA-CPT conjugate contributed to superior *in vivo* activity to the HT-29 colon and NCI-H460 lung carcinoma models, in contrast to free CPT [22]. The further study revealed that the conjugation of CPT with PGA altered drug pharmacokinetics, and increased drug accumulation in tumors based on the “enhanced permeability of tumor vessels and retention of macromolecules (EPR)” effects [27]. It is worth of noting that the combination between hydrophobic CPT and hydrophilic polymer contributes to the possibility of self-assembly. The formed micelles generally exhibited the decreased toxicity, and showed the potential of passive targeting to tumor tissue [23–25].

In this study, we synthesized the reduction-sensitive polymer-CPT conjugate by successively reacting azide-functionalized CPT and poly (ethylene glycol) methyl ether (mPEG) with alkyne focal groups in disulfide-linked poly (amido amine) (SS-PAA), and then fabricated the micelles to expectedly achieve the passive targeting to tumor tissue. Moreover, the effects of nanoencapsulation on the stability of its active form in physiological pH level and its cytotoxicity were evaluated. At last, the dithiothreitol (DTT) was used to simulate the different reduction conditions in body, and hence the drug release profiles together with the reduction degradation of the micelle were investigated.

2. Experimental part

2.1. Materials

Cystamine hydrochloride, propargyl amine, acryloyl chloride, poly (ethylene) methyl ether ($M_n = 1900$) and *p*-Toluesulfonyl chloride were purchased from Alfa Aesar and used as received. Dithiothreitol (DTT), Sodium azide, CuBr was obtained from Aladdin. 6-Bromohexanoic acid (98%), *N,N'*-dicyclohexylcarbodiimide (DCC) (99%), *N,N*-Diisopropylethylamine (DIEA), *N,N*-dimethylformamide (DMF), triethylamine, and dimethylamino pyridine (DMAP) were purchased from Sinopharm Chemical Reagent Co., Ltd. DMF was dried with 4 Å molecular sieve and redistilled before use. CPT, 5-diphenyltetrazolium bromide, MTT were obtained from Sigma–Aldrich.

2.2. Cell line and culture

Mouse muscular cell line L929 was supplied from Institute of Biochemistry & Cell Biology, Chinese Academy of Sciences. Cells were cultured in RPMI 1640 (Gibco BRL, Paris, France), supplemented with 10% fetal bovine serum (FBS, HyClone, Logan, Utah), streptomycin at 100 $\mu\text{g}/\text{mL}$, and penicillin at 100 U/mL. All cells were incubated at 37 °C in humidified 5% CO_2 atmosphere. Cells were split by using trypsin/EDTA solution when almost confluent.

2.3. Synthesis of *N,N'*-bis(acryloyl) cystamine (BAC)

BAC was synthesized according to the literature [28]. Cystamine dihydrochloride (10 mmol) was dissolved in a mixture of 15 mL of 3.5 M NaOH and 10 mL chloroform. This solution was heated up to 50 °C, and 5 mL of chloroform containing 20 mmol of acryloyl chloride was added dropwise under constant stirring over 15 min while the reaction temperature was maintained at 50 °C. After separating the phases while still warm, the aqueous phase was discarded. The remaining organic phase was cooled to room temperature, and the product precipitated directly from the solution. The white crystal product was recovered by filtration and recrystallized from chloroform to give a yield 50%.

2.4. Synthesis of disulfide-linked poly(amido amine) (SS-PAA)

As shown in Fig. 2, the SS-PAA was synthesized by the Michael addition polymerization between propargyl amine and BAC [29]. Firstly, BAC (2.60 g, 10 mmol) and propargyl amine (550.8 mg, 10 mmol) were added into a flask and dissolved in 20 mL MeOH. The solution was stirred at room temperature in the dark under nitrogen atmosphere for 7 days. Subsequently, 10 mol% excess propargyl amine was added into the reaction solution to consume

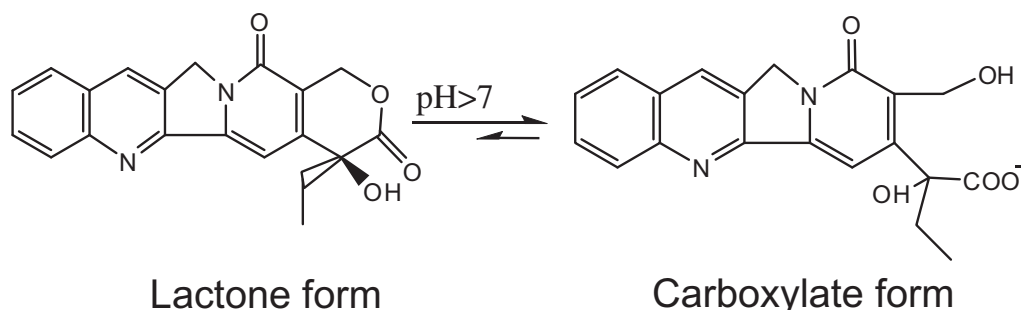


Fig. 1. Chemical structure of the two forms of CPT.

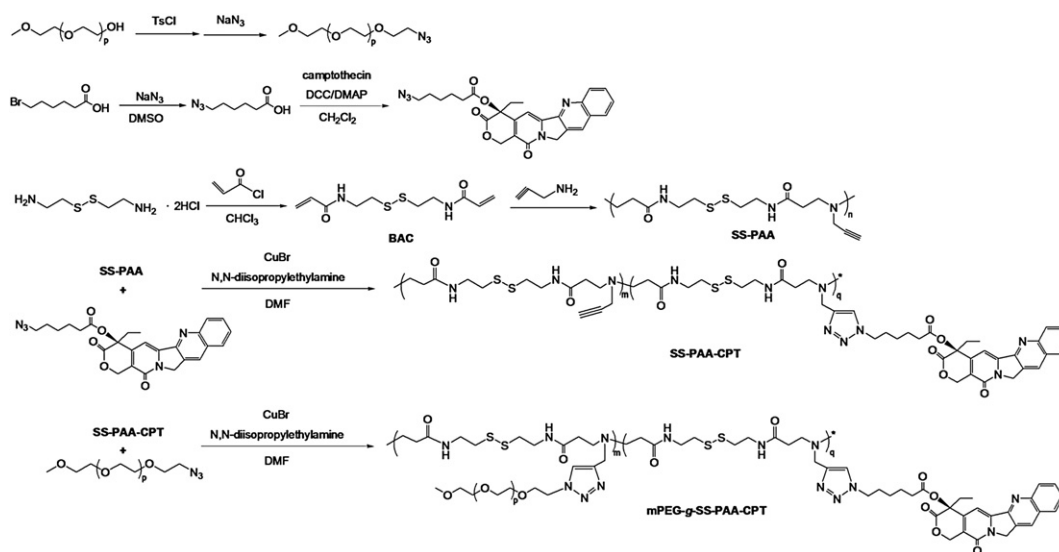


Fig. 2. Synthesis scheme of mPEG-g-SS-PAA-CPT conjugate.

any unreacted acrylamide groups, and the reaction was performed at room temperature for at least additional one week. At last, the reaction solution was evaporated, and then the residue was dried in vacuum at 40 °C to give the SS-PAA with alkyne focal groups.

2.5. Synthesis of mPEG-g-SS-PAA-CPT conjugate

mPEG-g-SS-PAA-CPT conjugate was synthesized by click reaction between alkyne focal groups in SS-PAA and azide-functionalized mPEG (mPEG-N₃) and CPT (CPT-N₃). Herein, the CPT-N₃ was synthesized from the CPT using a protocol same as that described by Emrick and Parrish [30], while mPEG-N₃ was prepared from mPEG according to the previous literature [31]. A representative procedure for the click conjugation is as follows: SS-PAA (315.46 mg, 1 mmol acetylene) and camptothecin azide (97.4 mg, 0.20 mmol) were dissolved in DMF in a small reaction vessel to target 20% camptothecin grafting. *N,N*-Diisopropylethylamine (DIEA) (51.7 mg, 0.4 mmol) and CuBr (57.4 mg, 0.4 mmol), were then added sequentially, and the reaction mixture was stirred in the dark at room temperature for 48 h. Then mPEG-N₃ (1.86 g, 0.96 mmol) was added into the reaction solution to consume the unreacted acetylene groups and the reaction was performed at room temperature for additional two days. After removal of solvent, the residue was dispersed in water, and thoroughly dialyzed against distilled water for 7 days using a dialysis membrane (MWCO: 7000 Da). The product was lyophilized to yield a slightly yellow solid of 1.81 g (90%), and labeled as mPEG-g-SS-PAA-CPT.

2.6. Micelle formation and critical micelle concentration

One milligram of mPEG-g-SS-PAA-CPT was dissolved in 8 mL of DMSO, and stirred at room temperature for 2 h, then dialyzed against de-ionized water for 48 h. The critical micelle concentration (CMC) was determined using pyrene as a fluorescence probe. The concentration of mPEG-g-SS-PAA-CPT conjugate was varied from 8×10^{-6} to 1 mg/mL and the concentration of pyrene was fixed at 6×10^{-7} mol/L. The fluorescence spectrum was recorded on F-4500 Fluorescence Spectrophotometer (Hitachi F-4500) with the excitation wavelength of 390 nm. The CMC was estimated as the cross-point when extrapolating the intensity ratio of I_{339}/I_{337} from low to high concentration regions.

2.7. Characterizations

¹H nuclear magnetic resonance (¹H NMR) spectra were recorded with a Bruker Avarice™ 500 NMR spectrometer. For NMR measurement, the sample concentration was 35 mg mL⁻¹ in CDCl₃ or DMSO-*d*₆.

FT-IR spectra were recorded on Nicolet Nexus 670 spectrometer. The samples were pressed into pellets with KBr. UV-Vis experiments were conducted on a UV-1900PC spectroscopy (Shanghai, China).

The molecular weights of mPEG-g-SS-PAA-CPT were measured with Agilent 1200 gel permeation chromatography (GPC) (Agilent Technologies Inc. Shanghai Branch). Agilent 1200 refractive index detector and aqueous SEC start-up kit were used. Chromatography columns (PL aquagel-OH MIXED columns, Polymer Laboratories Ltd. Amherst, MA, USA) were calibrated with poly (ethylene glycol) kit. The column temperature was maintained at 35 °C. Mobile phase was PBS buffer (0.137 M NaCl, 2.68 mM KCl, 3.2 mM Na₂HPO₄ and 1.5 mM KH₂PO₄, pH 7.4), and the flow rate was 1.0 mL/min.

The particle sizes and size distributions of mPEG-g-SS-PAA-CPT micelles were measured by dynamic light scattering (DLS) (Zetasizer Nano ZS, Malvern Instruments, UK).

Morphological observation of mPEG-g-SS-PAA-CPT micelles was performed using transmission electron microscopy (TEM). A copper grid with a carbon film was used. The copper grid was immersed in a drop of polymer solution for 60 s, and then dried at room temperature.

2.8. Degradation of mPEG-g-SS-PAA-CPT micelle

mPEG-g-SS-PAA-CPT micelle was degraded in the presence of water-soluble reducing agents, dithiothreitol (DTT) in PBS buffer [9]. The concentrations of DTT in mixture solution were set at 40 mM, 20 mM and 10 mM, respectively. In a typical procedure, mPEG-g-SS-PAA-CPT micelle (20 mg, 0.011 mmol disulfide) was treated with DTT in 27.5 mL PBS buffer under nitrogen at 37 °C. Aliquots were periodically withdrawn, diluted with PBS buffer at ambient temperature, and analyzed by GPC immediately to determine the extent of cleavage of the disulfide bonds in the copolymer. The size change of micelles was monitored by DLS measurement at different time intervals. Finally, the solution was dialyzed against

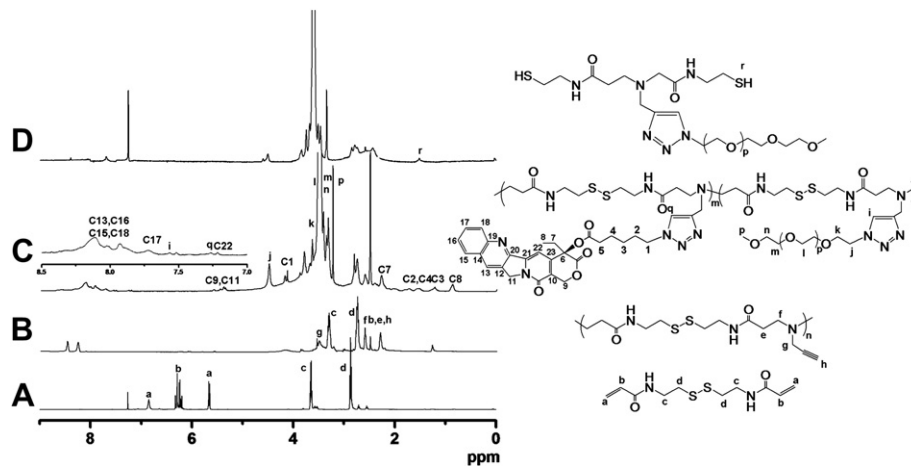


Fig. 3. ^1H NMR spectra of (A) BAC in CDCl_3 , (B) SS-PAA in $\text{DMSO}-d_6$, (C) mPEG-g-SS-PAA-CPT conjugate in $\text{DMSO}-d_6$ and (D) mPEG-g-PAA-SH in CDCl_3 .

distilled water for 7 days using a dialysis membrane (MWCO: 1000 Da) to remove the excess DTT. The lyophilized sample was characterized by ^1H NMR.

2.9. Stability of CPT in mPEG-g-SS-PAA-CPT micelle

To elucidate the stability of CPT lactone in mPEG-g-SS-PAA-CPT micelle over time at physiologic pH (7.4), the micelle was incubated in PBS buffer at 37°C at a concentration of 0.5 mg/mL. 1 mL aliquots were taken from the medium for monitoring by using a UV/vis spectrophotometry according to the method described by Zhao et al. [20]. The ratios (A_{324}/A_{345}) were calculated from the intensity of the characteristic UV absorption of CPT lactone form (λ_{max} : 324 nm) and carboxylate form (λ_{max} : 345 nm), and used to evaluate the stability of CPT lactone in mPEG-g-SS-PAA-CPT micelle.

2.10. Release profiles of CPT from micelle

Release of CPT from polymeric micelle was performed by the method described by Opanasopit et al. with minor modification [17]. The release profiles of CPT from mPEG-g-SS-PAA-CPT micelle were studied at $37 \pm 0.5^\circ\text{C}$ in three different media, i.e. 30 mL PBS buffer (7.4) with 10 mM and 40 mM DTT and neat PBS buffer (7.4) under constant stirring. 5 mg of free CPT or 10 mg of mPEG-g-SS-PAA-CPT were dissolved in a mixture of PBS (pH = 7.4) and DMSO (10:1). Five milliliter of each sample solution was charged into a dialysis tube (MWCO: 3500 Da). Then the dialysis tube was immersed in the dialysis medium. At certain time intervals, 0.6 mL aliquot of the dialysis medium was withdrawn, and the same volume of fresh media was added, respectively. The sample solution was analyzed by reverse-phase HPLC. Each experiment was carried out in triplicate. Means and corresponding standard deviations (mean \pm SD) were shown as results.

The concentrations of the drugs were assayed by reverse-phase HPLC (Agilent Technologies Inc. Shanghai Branch). Chromatographic separations were achieved using a Zorbax Eclipse XDB-C18 column at 35°C . The mobile phase was a mixture of triethylamine acetate (TEAA) buffer (0.1% v/v triethylamine, adjusted with glacial acetic acid to pH = 5.5)/acetonitrile with a ratio of 73:27 (v/v) for the assay of CPT. Mobile phase was delivered at a flow rate of 1.0 mL/min. Agilent 1200 UV/vis detector was set at 368 nm for CPT. The standard solution of CPT lactone and CPT-carboxylate were made by dilution of CPT stock solution in DMSO with pH = 3.5 and 12 PBS buffer, respectively. The analysis of CPT-carboxylate was

carried out 2 h after preparing the standard solution to ensure the complete conversion of CPT-lactone to CPT-carboxylate. Standard calibration samples were prepared at concentrations ranging from 0.1 to 50 $\mu\text{g}/\text{mL}$. The calibration curves exhibited linear behavior over the concentration range of about 3 orders of magnitude. The detection limits were evaluated on the basis of a signal-to-noise ratio of 3 and were 0.02 $\mu\text{g}/\text{mL}$ for CPT.

2.11. Cell viability assays

In vitro cytotoxicity of mPEG-g-SS-PAA-CPT conjugate and CPT to inhibit cells growth was determined by evaluation of the viability of mouse muscular cell line (L929) by MTT method. Cells were seeded in 96 well plates at an initial density of 6×10^3 cells/well in 100 μL growth medium and incubated for 24 h to reach 80% confluency at the time of treatment. Growth medium was replaced with 100 μL fresh serum-free media containing various amounts of mPEG-g-SS-PAA-CPT conjugate or CPT. Cells were incubated for 48 h. And then, the culture medium was replaced by 100 μL of MTT solution (0.5 mg/mL). After further incubation for 4 h in incubator, 100 μL of dimethyl sulfoxide (DMSO) was added to each well to replace the culture medium and dissolve the insoluble formazan-

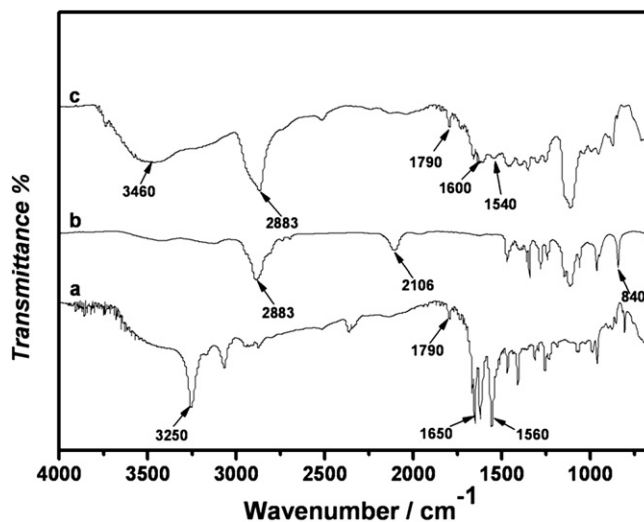


Fig. 4. FT-IR spectra (a) BAC, (b) mPEG-N₃, and (c) mPEG-g-SS-PAA-CPT conjugate.

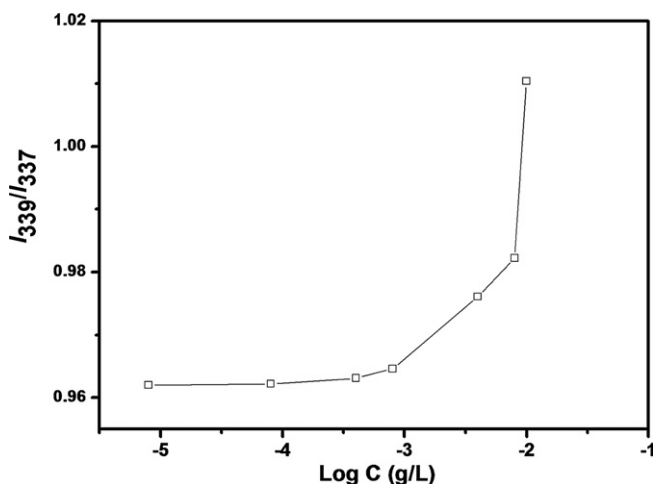


Fig. 5. I_{339}/I_{337} band intensity ratio of pyrene as a function of logarithm concentration of micelle.

containing crystals. The optical density (OD) was measured at 570 nm using an automatic BIO-TEK microplate reader (Powerwave XS, USA), and the cell viability was calculated from following equation:

$$\text{Cell viability (\%)} = \left(\frac{OD_{\text{sample}}}{OD_{\text{control}}} \right) \times 100 \quad (1)$$

where OD_{sample} represents an OD value from a well treated with samples and OD_{control} from a well treated with PBS buffer only. Each experiment was carried out in sextuplet. Mean and corresponding standard deviations (mean \pm SD) were shown as results.

3. Results and discussion

3.1. Synthesis of mPEG-g-SS-PAA-CPT conjugate

In this study, we report a water-soluble polymer-drug conjugate from functionalized mPEG, camptothecin (CPT) and reduction-degradable disulfide-linked poly(amido amine) (SS-PAA) by click chemistry as shown in Fig. 2. Firstly, the BAC monomer was synthesized according to a classic reaction pathway with acryloyl chloride under conventional Schotten–Baumann conditions. ^1H

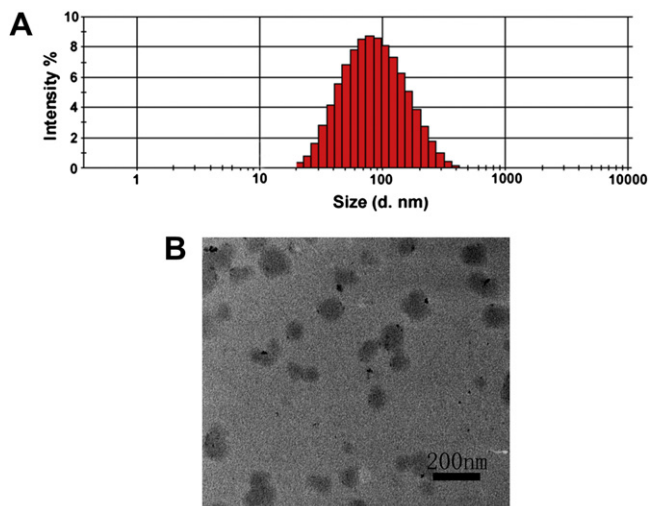


Fig. 6. (A) Size distributions, and (B) TEM photographs of mPEG-g-SS-PAA-CPT micelle.

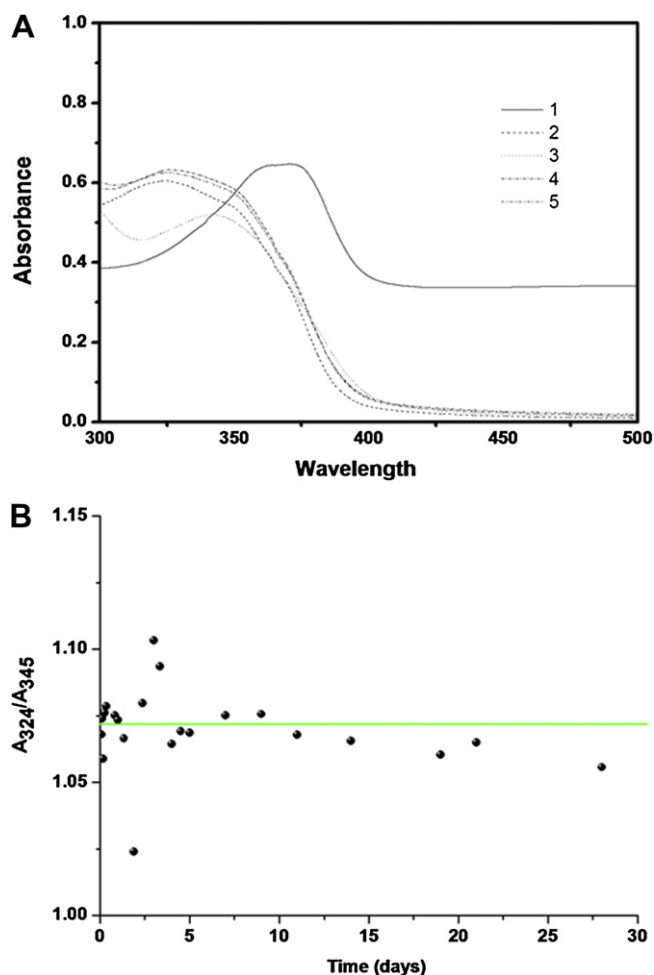


Fig. 7. (A) UV absorption curves of (1) CPT in pH 7.4 PBS, (2) mPEG-g-SS-PAA-CPT conjugate in pH 3.5 PBS, (3) mPEG-g-SS-PAA-CPT conjugate in pH 12 PBS, (4) mPEG-g-SS-PAA-CPT conjugate before incubation, and (5) mPEG-g-SS-PAA-CPT conjugate after 30-day incubation in pH 7.4 PBS at 37 °C; (B) A_{324}/A_{345} ratios of mPEG-g-SS-PAA-CPT micelle against incubation time in pH 7.4 PBS at 37 °C.

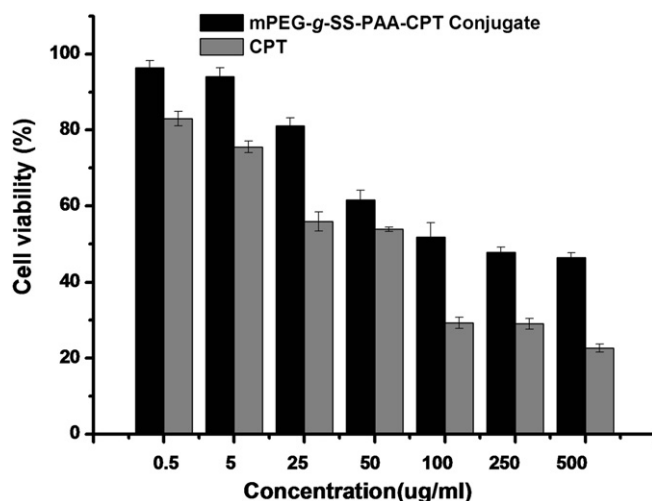


Fig. 8. Cell viability of mPEG-g-SS-PAA-CPT micelle at various CPT concentrations against L929 cell line for 48 h (mean \pm SD, $n = 6$).

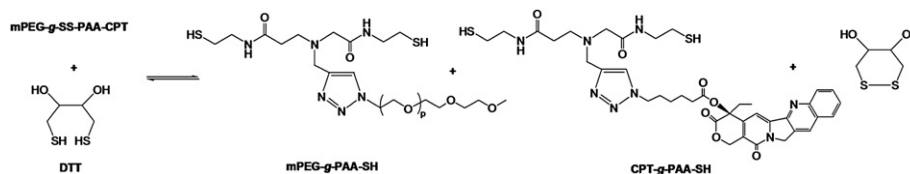


Fig. 9. Scheme of the reduction of mPEG-g-SS-PAA-CPT conjugate by DTT.

NMR confirmed the structure of BAC, and the detailed data of chemical shifts were shown in Fig. 3 A. The SS-PAA was synthesized by Michael addition of molar equivalents of the propargyl amine to BAC. The reaction was continued until the solution became viscous for magnetic stirring 7–10 days. Then, ca. 20 mol% excess of propargyl amine was added and the mixture was allowed to react for another 7 days to terminate the polymerization with amino end groups. The final structure of SS-PAA was confirmed by ^1H NMR (Fig. 3B). The signal at 2.23 ppm ($-\text{C}\equiv\text{C}-\text{H}$) indicated the presence of alkyne focal group. The molecular weight of SS-PAA measured by GPC (mobile phase: THF; standard sample: polystyrene) was about $M_n = 2.1 \times 10^4$, $M_w = 9.8 \times 10^4$. The inherent nature of Michael addition resulted in relatively high PDI of 4.67.

Coupling of acetylene-functionalized SS-PAA with azide-derived camptothecin was carried out using *N,N*-diisopropylethylamine (DIEA)/CuBr as catalyst in DMF at room temperature by targeting 20 mol% CPT incorporation (or one CPT per five monomer repeat units). Further grafting with mPEG is necessary to improve the water solubility of SS-PAA-CPT conjugate. Click cycloaddition of the residual acrylene groups with azide-terminated mPEG was performed by adding mPEG- N_3 into the reaction solution. The molecular weight of mPEG-g-SS-PAA-CPT conjugate measured by GPC was about $M_n = 5.9 \times 10^4$, $M_w = 3.8 \times 10^5$, and PDI = 6.44. The high PDI of SS-PAA, grafting degree of mPEG and conjugation probability of CPT resulted in high weight distribution of the mPEG-g-SS-PAA-CPT. ^1H NMR confirmed the structure of mPEG-g-SS-PAA-CPT conjugate, and the detailed data of chemical shifts were shown in Fig. 3C. The click reaction was confirmed from the appearance of new proton signals at 7.51 ppm (i, singlet) and 7.27 ppm (q, singlet) typical of methine proton of the triazole ring from the mPEG and CPT grafts, as well as the methylene protons at 4.53 (j, singlet) and 4.28 (C1) ppm adjacent to the triazole, respectively. The integral ratios of protons at 4.53 and 4.28 ppm were considered to suggest the conjugation probability of CPT and grafting extent of mPEG, in terms of percent monomers containing the conjugation with ca. 20% CPT and ca. 72% mPEG. The FT-IR spectra (Fig. 4) show a complete disappearance of the azide vibrational peak at 2106 cm^{-1} , and a new

absorption at about $1600\text{--}1640\text{ cm}^{-1}$ typical of triazole ring appeared. In addition, the mPEG-g-SS-PAA-CPT conjugate showed the intense stretching bands at 2883 cm^{-1} and 840 cm^{-1} for mPEG block, and a broad band $-\text{NH}$ at about $3200\text{--}3600\text{ cm}^{-1}$ for the SS-PAA.

3.2. Micelle formation

The mPEG-g-SS-PAA-CPT conjugate was found to be water-soluble and to form micelle in aqueous solution. The critical micelle concentration (CMC) was determined using pyrene as a probe. The plot of intensity ratio I_{339}/I_{337} of the pyrene excitation spectra against the logarithm of the micelle concentration is shown in Fig. 5. The CMC value can be determined at a micelle concentration of onset of I_{339}/I_{337} ratio increase. The mPEG-g-SS-PAA-CPT conjugate showed a CMC of ca. 0.003 mg/mL .

Dynamic light scattering (DLS) measurement shows that mPEG-g-SS-PAA-CPT conjugate formed micelle with sizes of ca. 88 nm (Fig. 6 A), suggestion of their efficient passive target potential to tumor tissue. TEM micrograph revealed spherical shapes and good dispersity with nanoscale sizes of 50 nm (Fig. 6B). The smaller size observed by TEM as compared to that measured by DLS, which might attribute to evaporation shrinkage of the PEG shell.

3.3. Stability of CPT in mPEG-g-SS-PAA-CPT micelle

As well known, the carboxylate conversion limits the bioavailability and the *in vivo* therapeutic efficacy of CPT, and thus, maintenance of the lactone structure is a prerequisite for an improved stability of CPT in mPEG-g-SS-PAA-CPT micelles. The characteristic UV absorption of mPEG-g-SS-PAA-CPT micelles was monitored in PBS (pH 7.4). As shown in Fig. 7 A, the maximum UV wavelength absorption (λ_{max}) of mPEG-g-SS-PAA-CPT in acidic media (pH = 3.5) and in basic media (pH = 12) located at 324 and 345 nm respectively, which represented the lactone and carboxylate form of CPT in mPEG-g-SS-PAA-CPT micelle [20]. However, the maximum UV absorptions of native CPT lactone and carboxylate forms were at

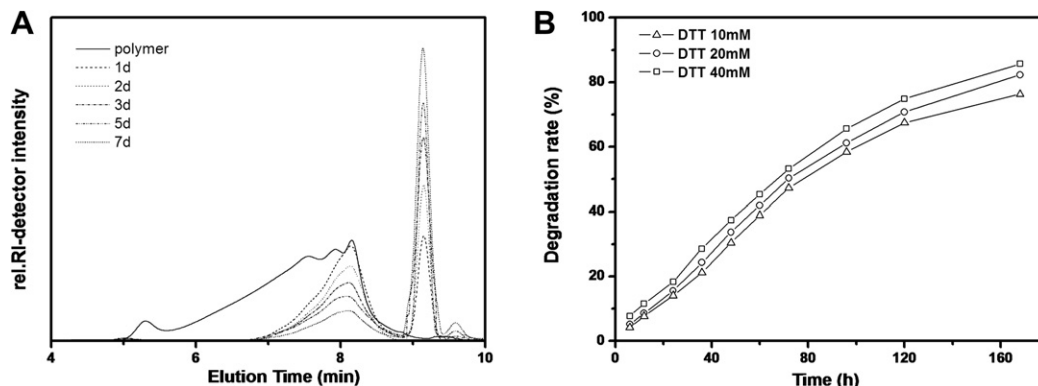


Fig. 10. (A) The molecular weight distribution of mPEG-g-SS-PAA-CPT conjugate in the incubation with 40 mM DTT in PBS buffer (pH = 7.4) at $37\text{ }^\circ\text{C}$; (B) The degradation rate of the copolymer in the incubation in the incubation with various DTT in PBS buffer (pH = 7.4) at $37\text{ }^\circ\text{C}$.

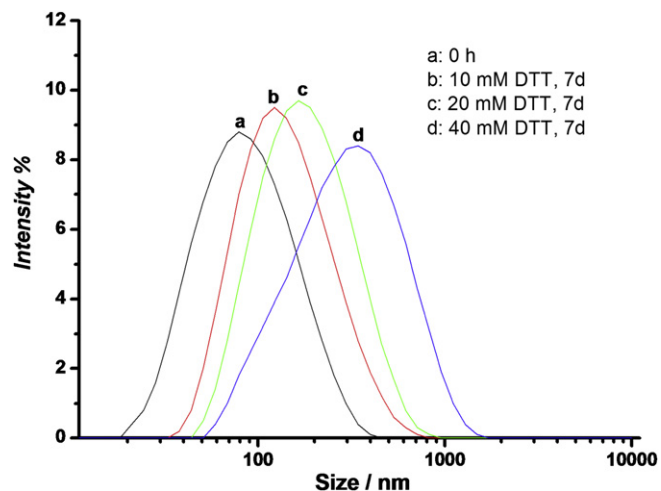


Fig. 11. The size change of mPEG-g-SS-PAA-CPT micelle in response to DTT in PBS buffer (pH = 7.4) determined by DLS measurement.

355 and 368 nm. That is to say, the conjugation of CPT with the SS-PAA resulted in a blue shift of the maximum UV absorption of lactone and carboxylate forms to 324 and 345 nm, respectively. So A_{324}/A_{345} ratios were calculated from the intensity of the maximum UV absorption of lactone and carboxylate forms of CPT, and used to evaluate the stability of CPT in mPEG-g-SS-PAA-CPT micelle as shown in Fig. 7B. The A_{324}/A_{345} ratios of mPEG-g-SS-PAA-CPT micelle surrounded an analogical value in agreement with experimental error in the whole incubation time (even in one month incubation). On the other hand, the lactone form of native CPT in PBS disappeared quickly. It was thought that the esterification of the 20-OH group of CPT was able to improve its stability. In addition, the micellization of mPEG-g-SS-PAA-CPT conjugate in aqueous medium was also beneficial for the enhancement of CPT stability [32].

3.4. Cytotoxicity of mPEG-g-SS-PAA-CPT micelle

The *in vitro* cytotoxicity of mPEG-g-SS-PAA-CPT micelle was evaluated with mouse muscular cell line (L929) by MTT assay. Representative concentration-growth inhibition curves showing the effects of treatment with mPEG-g-SS-PAA-CPT micelle on the growth of L929 after 48 h are shown in Fig. 8. Although both mPEG-g-SS-PAA-CPT micelle and CPT inhibited cell growth in a dose-dependent manner, the former was consistently less toxic than that of CPT. It was thought that the decreased cytotoxicity of mPEG-g-SS-PAA-CPT conjugate resulted from the slow release of CPT from the mPEG-g-SS-PAA-CPT micelle.

3.5. *In vitro* degradation of mPEG-g-SS-PAA-CPT Conjugate

The degradability of the mPEG-g-SS-PAA-CPT conjugate was investigated by the incubation of copolymers with DTT under physiological conditions. The disulfide bond was cleaved by DTT, which has been explained by the formation of more stable six-membered cyclic disulfide after the oxidation of such dithiol as shown in Fig. 9 [33]. ^1H NMR and GPC measurements confirmed the cleavage of disulfide bonds to yield mPEG-g-PAA-SH. The new proton signal at 1.5 ppm (τ , -SH) included the presence of thiol end-group and new format peaks at 2.75 ppm of ethylene protons next to the thiol end-group ($-\text{CH}_2-\text{SH}$) are shown in Fig. 3D while the signal at 2.92 ppm attributable to the methylene protons neighboring to disulfide bond ($-\text{CH}_2-\text{SS}-\text{CH}_2-$) completely disappeared. In addition, the changes of molecular weight distribution

of the copolymers are shown in Fig. 10A. The peak intensity of small molecules around 9 min of elution time increased together with the decrease of peak intensity of polymer fraction with high molecular weight, indicating that the copolymer degraded as smaller segments. At a longer incubation time (i.e. up to 7 d), most of the copolymers were broken into oligomers and small complexes. The GPC trace indicated that the degraded segments had $M_n = 2.35 \times 10^3$, $M_w = 2.47 \times 10^3$ and PDI = 1.05. The degradation rate of the copolymer increased with an increase in the amount of DTT as shown in Fig. 10B. When the concentration of DTT was 40 mM, over 85% copolymer was degraded in 7 d. The degradation rate of the copolymer was slower than those of previous reports [4], which might be ascribed to the steric hindrance of grafted mPEG and conjugated CPT.

The size change of micelle in response to DTT in PBS buffer (pH = 7.4) was traced by DLS measurement as shown in Fig. 11. Notably, aggregation of micelle occurred in present of DTT and the size increased from 87 nm to 350 nm after 7 d when the concentration of DTT was 40 mM. Furthermore, the micelles size increased with an increase of the DTT concentration. The aggregation of micelle might be ascribed to the reductive cleavage of the internal disulfide bonds, which changed the hydrophilicity–hydrophobicity equilibrium for the original assembly of the copolymer.

3.6. Release of CPT from micelle

Since the CPT was conjugated to the reduction-degradable polymer via hydrolysable ester bonds, it was believed that the CPT could be released from mPEG-g-SS-PAA-CPT prodrug by the hydrolysis of ester bonds. As shown in Fig. 12, the free CPT drug was nearly completely released during 24 h. Compared with free CPT, the accumulative drug release behaviors of mPEG-g-SS-PAA-CPT micelle in the absence of DTT showed slow gradual profiles, 18.6% of CPT was released in 14 days due to the hydrolysis of ester bonds between CPT and polymer backbone, suggesting its sustained drug release behaviors. Interestingly, CPT was rapidly released from the mPEG-g-SS-PAA-CPT micelle in the presence of DTT. For example, ca. 66% CPT was released in 14 days. It was thought that the structure of mPEG-g-SS-PAA-CPT micelle was destroyed due to the degradation of disulfide bonds in polymer backbone under a reduction environment, which resulted in the enhanced hydrolysis of ester bonds between CPT and polymer backbone. This was in line with the results that the mPEG-g-SS-PAA-CPT conjugate was degraded and the micelle was destabilized in the presence of DTT.

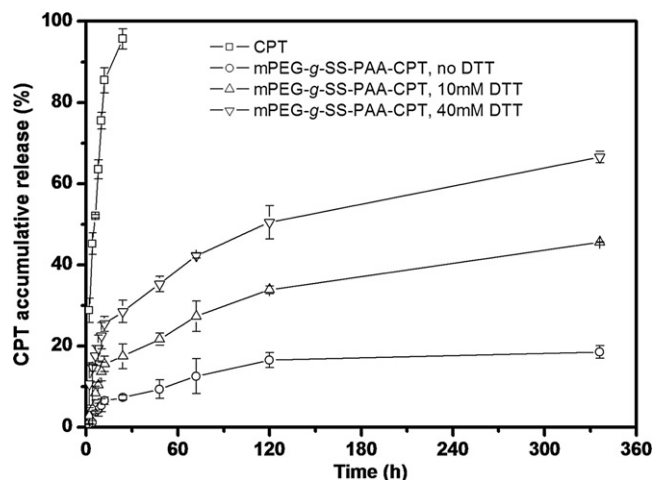


Fig. 12. *In vitro* release profiles of CPT from free drug and mPEG-g-SS-PAA-CPT micelle in pH 7.4 PBS at 37 °C (means \pm SD, $n = 3$).

Although the enhanced hydrolysis of ester bonds between CPT and polymer backbone could produce faster drug release, the hydrolysis of ester bonds was still much lower than the cleavage of disulfide bonds in the presence of DTT. At the same time, the AA-CPT monomer also released when the depolymerization extent of main chains is very high. As a result, the release of CPT was lower than the polymer degradation rate.

4. Conclusions

A reduction-degradable mPEG-g-SS-PAA-CPT conjugate was synthesized, which was fabricated as spherical micelle with size of ca. 88 nm. It was found that the copolymer was degradable by incubation with DTT. The biodegradation of mPEG-g-SS-PAA-CPT conjugate due to reductive cleavage of disulfide bonds can facilitate rapidly release of CPT from the micelle. Compared to CPT, mPEG-g-SS-PAA-CPT micelle showed improved aqueous solubility and stability for CPT, gradual drug release profiles, and essential decreased cytotoxicity, suggesting their great potentials as anti-tumor polymer prodrugs.

Acknowledgements

The research work was supported by the 973 Projects of Chinese Ministry of Science and Technology (2009CB930300), National Natural Science Foundation of China (50873080), Shanghai Municipality Commission for Special Project of Nanometer Science and Technology (0952nm05300), Shanghai Municipality Commission for Non-governmental International Corporation Project (09540709000) and International Corporation Project (10410710000), Foundation for New Century Excellent Talents in University of Ministry of Education of China (NCET-10-0435), and Fundamental Research Funds for the Central Universities (Self-Determined and Innovative Research Funds of WUT 2010-II-022 and JUSRT30905).

References

- [1] Bajpai AK, Shukla SK, Bhanu S, Kankane S. *Prog Polym Sci* 2008;33(11):1088–118.
- [2] Rapoport N. *Prog Polym Sci* 2007;32(89):962–90.
- [3] Wei H, Cheng SX, Zhang XZ, Zhuo RX. *Prog Polym Sci* 2009;34(9):893–910.
- [4] Meng F, Hennink WE, Zhong Z. *Biomaterials* 2009;30(12):2180–98.
- [5] Gabizon AA, Tzemach D, Horowitz AT, Shmeeda H, Yeh J, Zalipsky S. *Clin Cancer Res* 2006;12(6):1913–20.
- [6] Cuchelkar Vaikunth PK, Kopecek J. *Macromol Biosci* 2008;8(5):375–83.
- [7] Oh JK, Siegwart DJ, Matyjaszewski K. *J Am Chem Soc* 2007;129(18):5939–45.
- [8] Oh JK, Siegwart DJ, Matyjaszewski K. *Biomacromolecules* 2007;8(11):3326–31.
- [9] Sun H, Guo B, Cheng R, Meng F, Liu H, Zhong Z. *Biomaterials* 2009;30(31):6358–66.
- [10] Xu Y, Meng F, Cheng R, Zhong Z. *Macromol Biosci* 2009;9(12):1254–61.
- [11] Wall ME, Wani MC, Cook CE. *J Am Chem Soc* 1996;88(16):3888–90.
- [12] Rothenberg ML. *Ann Oncol* 1997;8(9):837–55.
- [13] Kingsbury WD, Boehm JC, Jakas D. *J Med Chem* 1991;34(1):98–107.
- [14] Berrada M, Serreqi A, Dabbarh F. *Biomaterials* 2005;26(14):2115–20.
- [15] Mi Z, Burke TG. *Biochemistry* 1994;33(42):12540–5.
- [16] Mi Z, Burke TG. *Biochemistry* 1994;33(34):10325–36.
- [17] Opanasopit P, Yokoyama M, Watanabe M. *J Control Release* 2005;104(2):313–21.
- [18] Fassberg J, Stella VJ. *J Pharm Sci* 1992;81(7):676–84.
- [19] Cao Z, Harris N, Kozielski A, Vardeman. *J Med Chem* 1998;41(1):31–7.
- [20] Zhao H, Lee C, Sai P. *J Org Chem* 2000;65(15):4601–6.
- [21] Fleming AB, Haverstick K, Saltzman WM. *Bioconjugate Chem* 2004;15(6):1364–75.
- [22] Bhatt R, Vries PD, Tulinsky J. *J Med Chem* 2003;46(1):190–3.
- [23] Cheng JJ, Khin KT, Jensen GS, Liu A, Davis ME. *Bioconjugate Chem* 2003;14(5):1007–17.
- [24] Yurkovetskiy AV, Hiller A, Syed S. *Mol Pharm* 2004;1(5):375–82.
- [25] Caiolfa VR, Zama M, Fiorino A. *J Control Release* 2000;65(12):105–19.
- [26] Fan NQ, Duan KL, Wang CY, Yu JH, Huang J. *Colloids and Surf B Biointerfaces* 2010;75:543–9.
- [27] Maeda H, Wu J, Sawa T. *J Control Release* 2000;65(12):271–84.
- [28] Yu H, Grainger DW. *Macromolecules* 1994;27(16):4554–60.
- [29] Lin C, Blaauboer CJ, Timoneda MM, Lok MC, Engbersen JFJ. *J Control Release* 2008;126(2):166–74.
- [30] Parrish B, Emrick T. *Bioconjugate Chem* 2007;18(1):263–7.
- [31] Hua C, Peng SM, Dong CM. *Macromolecules* 2008;41(18):6686–95.
- [32] Chang YC, Chu IM. *Eur Polym J* 2008;44(11):3922–8.
- [33] Tsarevsky NV, Matyjaszewski K. *Macromolecules* 2002;35(24):9009–14.